National Institute for Public Health
and the Environment
Ministry of Health, Welfare and Sport

WAGENINGEN
UNIVERSITY & RESEARCH

Bofei Li (950218515090)

Inverse Modeling of Ammonia in the Netherlands



Supervised by Maarten Krol, Ferd Sauter (RIVM) and Addo van Pul (RIVM)

MSc Thesis Environmental Science

Wageningen University

2020

ACKNOWLEDGEMENTS

The author would like to acknowledge his supervisors, Maarten Krol from Wageningen University and Research (WUR), Ferd Sauter, and Addo van Pul from the National Institute for Public Health and Environment (RIVM), for their instruction of this research strategy and the background knowledge. I also thank them for their supports during the experiment running and the encouragements when I was in troubles. I thank Reinder Ronda and all the other colleagues in the Meteorology and Air Quality department (MAQ) group who gave help for programming, documents and feedbacks in the thesis rings. I thank the colleagues in RIVM for the data and background information.

ABSTRACT

Ammonia is an important pollutant in the atmosphere. It is the precursor gas of secondary particulate aerosol and an indicator of local emission. With large areas of grassland and crop field, the Netherlands has the highest ammonia concentration in Europe. In this research, the OPS (Operational Priority Substances) model is used to simulate the atmospheric NH_3 concentration in the Netherlands based on the emission data in 2018. The emission sources are analyzed in different categories and other factors like transportation from outside are also in consideration. The emission estimate is optimized by the inverse modelling method. According to the result, the OPS model has a quite acceptable simulation performance. The agricultural sources are proved to be dominant. The emission from stables is likely to be overestimated. On the contrary, emission sources from the cropland (including manure application and crop emission and fires) are expected to be underestimated and the contribution to the average NH_3 concentration is relatively low. Factors like manure application methods or changing numbers of animals explain the high emission uncertainty. Large misestimation also occurs in the transportation from surrounding countries. Different bias correction and model error selection can influence model performance as well. More research is needed in the future, for example the temporal variation modelling and spatial distribution of emissions.

Table of Content

Acknowledgements i
Abstract ii
LIST OF FIGURES iv
LIST OF TABLES vi
1. Introduction 1
1.1 Research Background 1
1.2 Research Objective 6
1.3 Research Questions 6
2. Methodology 6
2.1 OPS Model 7
2.2 Inverse Modeling Method 9
2.3 Experiment Design 12
3. Result 15
3.1 Emission Analysis 15
3.2 OPS Simulation 16
3.3 Model Optimization 20
4 Discussion 25
4.1 Result Analysis 25
4.2 Future Study 28
5. Conclusion 30
6. Reference 32
Appendix I. Code of emission categories 35
Appendix II. Emission and Concentration for Each Category 36
Appendix III. Python Script for Emission Estimate Optimization 38

LIST OF FIGURES

Figure 1 Trends in reported ammonia emissions and measured NH_3 between 1990 (emissions)/1993(measurements) and 2014. The ammonia concentration is represented by the mean of gap filled time series of 8 monitoring stations (Jimmink et al., 2015). 3

Figure 2 Contribution of different NH_3 emission sources to the total ammonia emission in the Netherlands from 1990 till 2017 (emissieregistratie.nl). 4

Figure 3 Trends in reported ammonia emissions and concentration in recent years. The blue line in decline is the modelled NH_3 emission; the green and purple lines are the measured and modelled atmospheric concentration respectively (emissieregistratie.nl). 5

Figure 4 Schematic view of the long term and short-term OPS models with its pre-processing steps by the programs MPARKNMI and METPRO. Note that most users will only use the OPS-LT part in the red box. 7

Figure 5 Locations of MAN and LML measuring points in the Netherlands (RIVM, www.luchtmeetnet.nl). White dots: NH_3 concentration, green dots: NO_x concentration, blue dots: wet deposition NO_y, NH_x, red dots: dry deposition NH_3. 9

Figure 6 The building of Jacobian Matrix K. According to the linearity of the model, the column Ki equals to the corresponding contribution concentration $Ccontr, i$, $Ki = Ccontr, i$. 11

Figure 7. Emission of NH_3 in the Netherlands (right) and the sea and the surrounding countries (left), in 2017. 15

Figure 8 Each category's ammonia emission rate within the Netherlands. 16

Figure 9 Scatter plots between the simulation and the observation of MAN measurement system (blue points) and LML measurement system (orange points) in 2018. The red line is the 1:1 reference line. 17

Figure 10 Modelled NH_3 concentration at measurement stations in the Netherlands in 2018 (in $\mu g/m3$). The points are located where the stations are. 18

Figure 11 Original (left) and optimized (right) scatter plots between the simulation and the observation of MAN measurement system (blue points) and LML measurement system (orange points). The red line is the 1:1 reference line. 21

Figure 12 The relative changes in the emission estimate and error. The original value of all categories was 1 (the red line) and the optimal estimate values

were the heights of the columns. The red error bars were the corresponding original emission errors and the black error bars were the error after reduction. 22

Figure 13 Dominant land use for the Netherlands and for Belgium and Germany (Sauter *et al.*, 2018). 26

Figure 14 The annual percentage of hours in which the mean wind direction is from each of the four cardinal wind directions (based on a statistical analysis of historical hourly weather reports and model reconstructions from January 1, 1980 to December 31, 2016 observed in Amsterdam)(*Weather Spark*).27

LIST OF TABLES

Table 1 Relative emission error of each category (Lagerwerf *et al.*, 2019). One standard deviation is used for this study. 14

Table 2 Emission percentage of each category, and after deposition, chemical reaction and in- and out-fluxes, the concentration percentage originated from each category. The NH_3 concentration from outside is the result of transportation. 19

Table 3 Emission amount of each category and its uncertainty before and after the optimization 22

Table 4 Optimizing results before and after bias correction 23

Table 5 Optimized estimate (emission multipliers) with the model error of 1, 2 and 0.6 $\mu g/m3$. 24

1. INTRODUCTION

1.1 Research Background

In the past decades, ammonia (NH_3) has drawn more attention as an important atmospheric pollutant that is mainly from agricultural activities, together with waste disposal and vehicular exhaust (Behera *et al.*, 2013). As a reduced form of nitrogen, ammonia after emission is subsequently mixed with oxidized acid gases (NO_x or SO_2) and transported in the atmosphere. It is chemically transformed into secondary inorganic aerosols such as ammonium nitrate (NH_4NO_3) and ammonium sulfate ($(NH_4)_2SO_4$) and other NH_3 fractions are removed from the atmosphere by dry and wet deposition. The deposited NH_3 back to the surface can cause acidifying and eutrophying effects on terrestrial and aquatic ecosystems (Bobbink *et al*, 1998) and the secondary products in particulate matter lead to detrimental effects on public health (Schlesinger and Cassee, 2003, Buijsman *et al.*, 1998).

The reaction between NH_3 and acid can be in different forms. As a result, reductions in SO_2 and NOx emissions influence the formation of ammonium salts and consequently, the ammonia concentration in the air. This phenomenon has been observed in several European countries (Sutton *et al.,* 2003). Previous studies indicate aerosol formation is more often limited by HNO_3 ,especially in wintertime (Womack *et al.*, 2019). However, some researches reveal that the particle matter formation can be equally sensitive to NH_3 concentration. Taking different opinions into account, the aerosol can be more effectively controlled by reducing either NH_3 or acid gases based on research and modelling (Franchin *et al.*, 2018).

According to Loubet *et al.* (2009), a large fraction of the emitted NH_x (ammonia and ammonium) may be recaptured by the surrounding vegetation, hence reducing the contribution of these hot spots to long-range transport of NH_x. Local recapture of NH_3 ranges from 2% to 60% within 2 km of a hot spot. The main means of NH_3 wet deposition is the in-cloud scavenging process. When the plume is mixed into the clouds, NH_x is transferred into cloud droplets. These droplets aggregate through various microphysical processes to snowflakes and raindrops, which are then deposited from the atmosphere. In the areas with low emission, the wet deposition during transportation from outside is the main sink of NH_3. In the countries with high NH_3 emission densities as the Netherlands, dry deposition of NH_3 from local sources and wet deposition of ammonium (NH_4^+) from remote sources dominate the deposition (Asman *et al.*, 1998).

Meteorological processes influence the effectiveness of the previously mentioned processes (Bleeker *et al.*, 2009). Local dry deposition is sensitive to source height, atmospheric stability, wind speed, structure of the surrounding canopies. Other factors are like stomatal absorption, which mainly depends on green leaf area index and stomatal NH_3 compensation point of vegetation, and , absorption at leaf and soil surface , which depends largely on surface wetness (Loubet *et al.*, 2009). Long-distance transportation and wet deposition are also influenced by meteorological factors like precipitation and wind direction.

Ammonia and ammonium are both widely studied. However, the measurements of NH_3 are more suitable to be the indicators of emission, because NH_4^+ is, the product of NH_3 and acids, which is more sensitive to the concentration of acid gas. For example, the rapid decline in SO_2 concentrations has an influence on the ammonium trend (Sutton *et al.*, 2003, Horvath and Sutton, 1998). Besides, the atmospheric lifetime of NH_4^+ is longer than that of NH_3. As a result, the foreign emissions of ammonium have generally a larger effect on the Dutch concentrations (van Zanten *et al.*, 2017). According to the model results of van der Swaluw *et al.* (2011), 50% of NH_4^+ suspending in the air and 40% of NH_x (NH_3 and NH_4^+) in droplets are from sources outside of the Netherlands. In contrast, only around 15% of NH_3 is imported from abroad (the number is higher in the border areas near Germany and Belgium). Therefore, the NH_3 concentration in the atmosphere is considered as the most reliable component to monitor the long-term tendency of the emission (Bleeker *et al.*, 2009).

Ammonia in the Netherlands

In the Netherlands, ammonia concentrations are the highest in Europe due to a high density of agricultural activities (van Zanten *et al.*, 2017). Among the total ammonia emission, about 85% comes from agricultural sources; other emissions are from the industry, traffic and consumers (emissieregistratie.nl).

The national government has made policies for ammonia reduction for decades. For example, a ban on manure surface spreading came into force in 1991, making it mandatory to inject the manure into the soil either directly or shortly after application. To a large extent, this policy prevented the emission of NH_3 after the application of animal manure. Provinces are also responsible for the implementation of nature policies and the regulation of ammonia emission close to nature areas (Luesink and Michels, 2018). At the continental level, the European Parliament and the Council of the European Union have set national emission ceilings (NEC) for the pollutants to

prevent acidification and eutrophication. Ammonia is included in order to provide more comprehensive protection for the environment and human health from their adverse effects (EU, 2001).

As a result of the ammonia abatement policies, reported ammonia emissions show a steady decline since 1990 with the largest decline in the first decade (Figure 1). The decline is largely due to the measure of incorporating animal manure into the soil instead of broadband spreading (van Zanten *et al.*, 2017). The plots can be generally distinguished into two periods: a period between 1993 and 2004 when ammonia concentrations were declining and a period of slightly increasing ammonia concentrations from 2005 and afterward. In the first period, large emission reductions were reported, while the second period is characterized by smaller emission reductions (Wichink Kruit *et al.*, 2017).

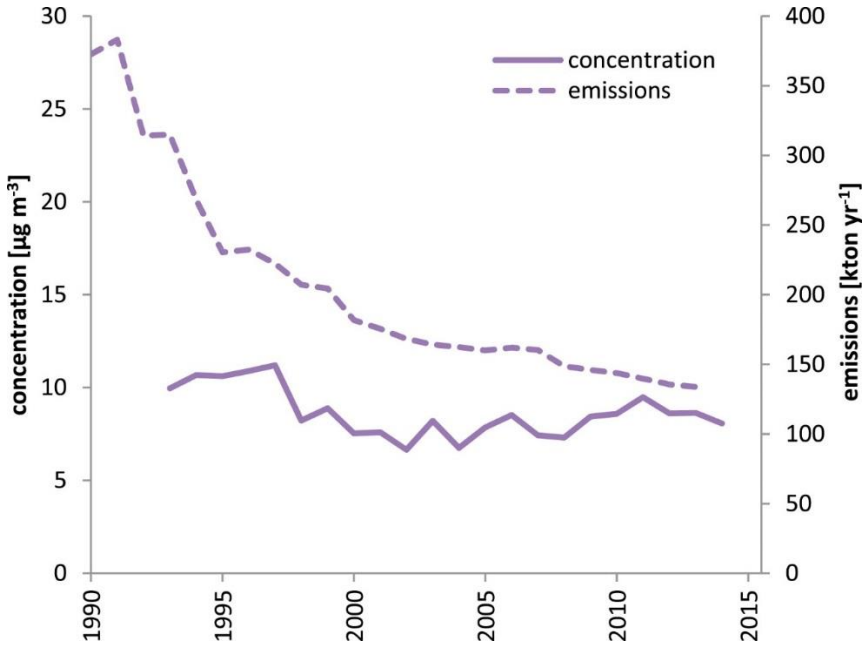


Figure 1 Trends in reported ammonia emissions and measured *NH_3* between 1990 (emissions)/1993(measurements) and 2014. The ammonia concentration is represented by the mean of gap filled time series of 8 monitoring stations (Jimmink et al., 2015).

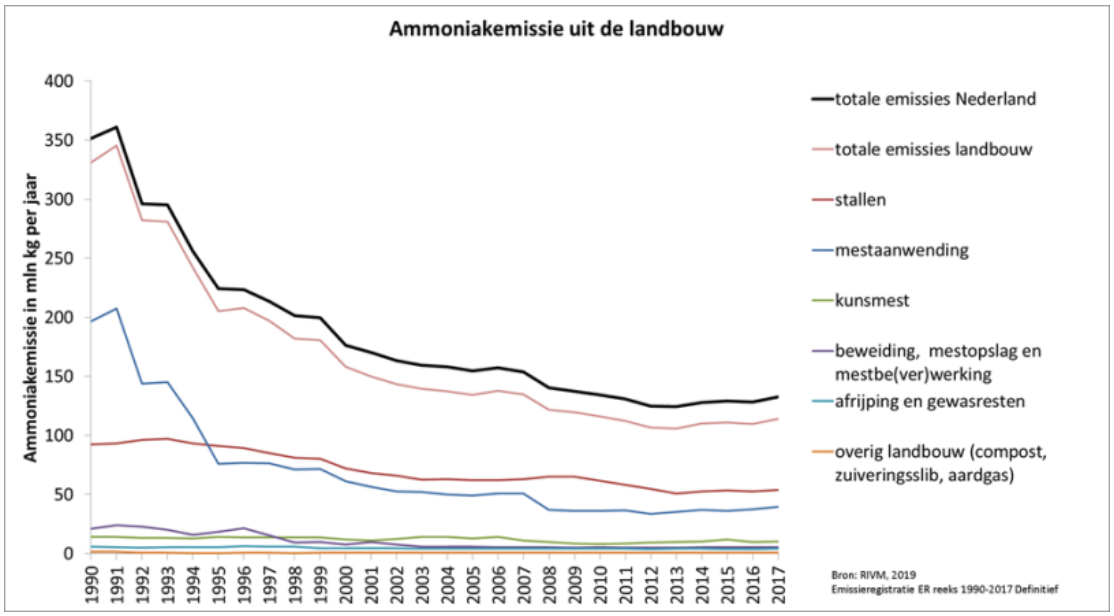


Figure 2 Contribution of different NH_3 emission sources to the total ammonia emission in the Netherlands from 1990 till 2017 (emissieregistratie.nl).

Low-emission manure spreading techniques have an important reducing effect on the atmospheric ammonia concentration. Figure 2 shows the reported emission changes from some major sources in the past decades. Without these techniques, the ammonia concentrations at the measurement stations would have been 3.5–4 µg m^{-3} higher in recent years (Wichink Kruit *et al.*, 2017). Declining trends are also found for other agricultural emission sources like stable animals and manure storage.

Compared with the reported emission reduction, the NH_3 concentration decreases far slower. Focusing on the data of recent years in Figure 3, the emission (blue line) continues in decline while the concentration has even a tendency of increasing for both the modeled (purple) and measured values (green). A difference around 10% is also observed between the modelling and the measurement. Therefore, there is a necessity to check the NH_3 emission reduction and to simulate the concentration more accurately.

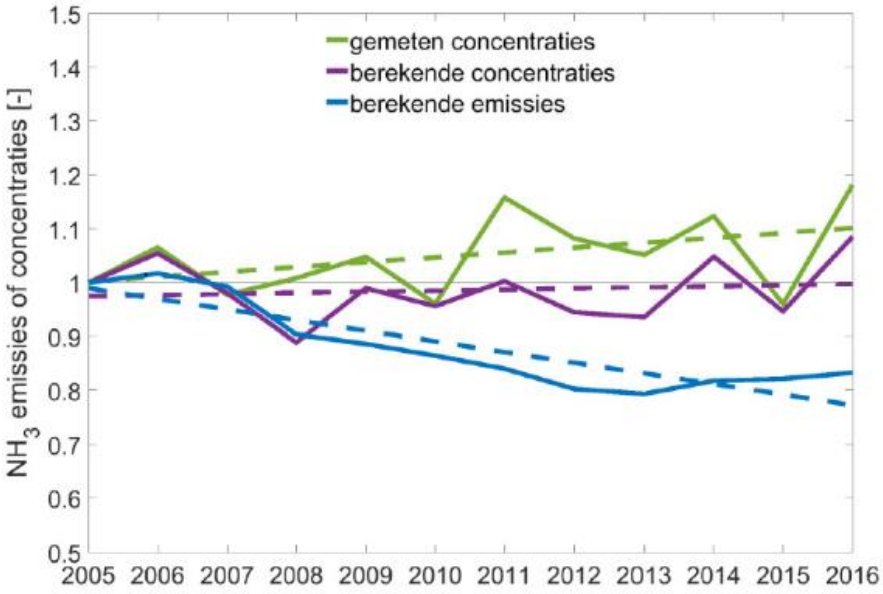


Figure 3 Trends in reported ammonia emissions and concentration in recent years. The blue line in decline is the modelled *NH_3* emission; the green and purple lines are the measured and modelled atmospheric concentration respectively (emissieregistratie.nl).

The OPS Model

With the help of computers, air quality models can provide pollutants information in space and time (Fahey *et al.*, 2017). The OPS (Operational Priority Substances) model is used in this research. The model simulates the atmospheric process sequence of emission, dispersion, transport, chemical conversion and deposition. Details about the model's mechanism is described in the following chapter. Several previous studies have been performed using OPS. In Wichink Kruit *et al.* (2017), a detailed analysis of the trend in *NH_3* using the OPS model is presented. The general performance of the OPS model for ammonia concentration, ammonium concentration and wet deposition of ammonia and ammonium is quite good when evaluated with observations over the whole period.

From the knowledge above we find that emissions declined at a much lower rate since 2005 but the observed concentrations increased slightly. One-third of the observed difference in trends can again be explained by the changed chemical conditions while for the rest the explanation is uncertain (Wichink Kruit *et al.*, 2017).

In this research, I investigate relations between the emission and the atmospheric NH_3 concentration in 2018, the Netherlands, by modeling different emission cases in order to optimize the emission estimation and find explanation for the under- or overestimation. Finally, I will give recommendation for further model improvement.

1.2 Research Objective

To investigate the relations between ammonia emission and its atmospheric concentration in the Netherlands.

1.3 Research Questions

General research question:

What are the effects of changes in the input or model parameters of the OPS model on the ammonia concentration and deposition?

Specific research questions:

- Compared with the observed ammonia concentration, how does OPS perform based on the emission data, in a one-year modeling study?
- Do the ammonia concentration and emission in the Netherlands have a linear relationship, in the one-year OPS modeling?
- What is the emission matrix, which presents how the change of each emission source category affects the concentration?
- Can we improve the comparison between modeled concentrations and measured ones by changing emissions (within certain boundaries)?
- What is the role of other processes (chemistry, deposition, foreign contribution) in the relation between emission and atmospheric concentration?

2. METHODOLOGY

First, a review of the OPS model description manual (version 4.5.2) (Sauter *et al.*, 2018) is conducted to describe the basic information about the OPS model, in preparation for the running of experiments. Previous studies also provide experience about OPS modeling, knowledge about pollutants in the Netherlands, and mechanisms of ammonia in the atmosphere. A description of inverse modeling is also given to present the statistical approaches that are used for data analysis. In the last step, I present a step-by-step analysis of the numerical experiments I conducted during my thesis research.

2.1 OPS Model

The OPS model used in this research is aiming to calculate the concentration and deposition of pollutants for the Netherlands using a high spatial resolution (typical $1 \times 1\ km^2$). The substances simulated by OPS can be divided into three groups: The acidifying and eutrophying substances (SO_2, NO_x, NH_3 and secondary products), non-acidifying (gaseous) substances and particle-bounded substances.

As shown in Figure 4, the flow chart describes the operation overview of the model. Schematically, it consists of three main parts.

a. A primary pre-processor MPARKNMI that reads hourly meteorological observations and interpolates these observations to 6 meteorological regions in the Netherlands.

b. A secondary pre-processor METPRO that calculates transport trajectories arriving at a receptor on the basis of hourly wind observations. METPRO also derives secondary parameters, which define the atmospheric state along the trajectories from the observed data. This pre-processor classifies hourly meteorology data into groups with similar properties and, in this way, describes the necessary statistics for the relevant period.

c. The OPS-model itself, which computes concentrations and depositions on the basis of various inputs.

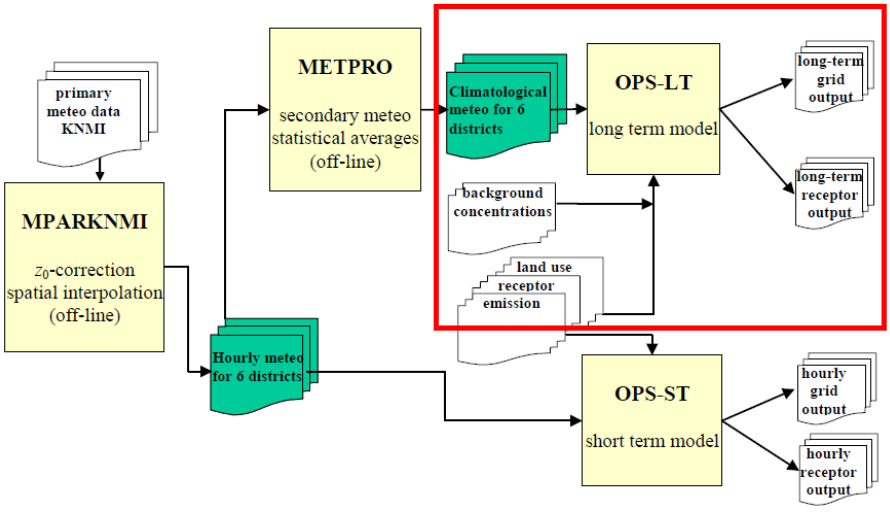


Figure 4 Schematic view of the long term and short-term OPS models with its pre-processing steps by the programs MPARKNMI and METPRO. Note that most users will only use the OPS-LT part in the red box.

The approach used in this research for the OPS-model can be classified as a long-term climatological trajectory model in combination with a Gaussian plume model on the local scale (typically <30 km) which treats impacts of sources on a receptor independently. The model is basically a linear model. In other words, it can be treated as a pseudo non-linear model because the chemical reaction rates and dry deposition velocities rely on the background concentration of pollutants (Sauter *et al.*, 2018).

The input data of the model includes the information about receptors and emission sources (for example coordinates, emission strength, height, horizontal dimensions, etc.) and information about the meteorological conditions measured at one or more locations in the Netherlands (including wind direction and wind speed at two heights, precipitation data, global radiation, temperature and snow cover.) The output of the model consists of concentration, dry deposition and wet deposition data, listed either by receptor or in gridded form.

Receptors information

Receptors are located at measurement points of MAN (Meetnet Ammoniak in Natuurgebieden, man.rivm.nl), which has 217 NH_3 observation points and LML (Landelijk Meetnet Luchtkwaliteit, www.luchtmeetnet.nl) with 8 measurement stations (Figure 5). Information like the measurement stations, locations and receptors heights are parts of the input in the OPS model while the measured concentrations at the receptors are also used as the observation data for the model optimization.

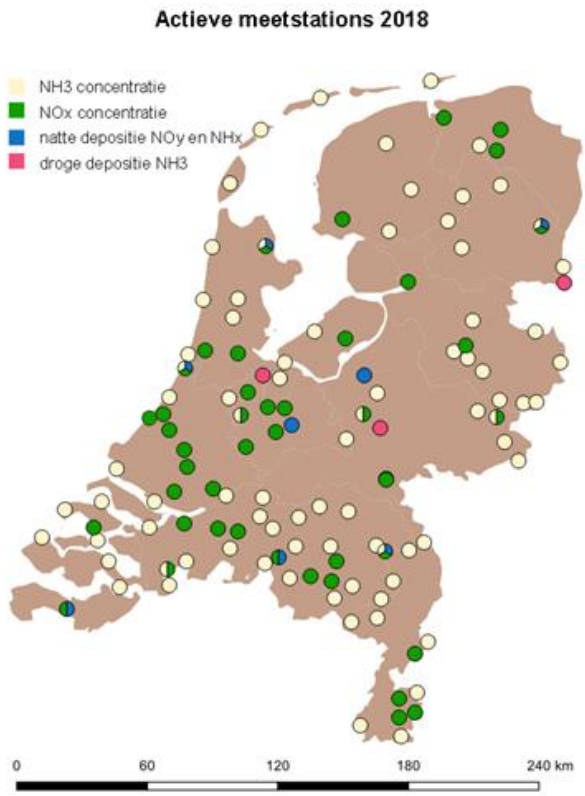


Figure 5 Locations of MAN and LML measuring points in the Netherlands (RIVM, www.luchtmeetnet.nl). White dots: NH_3 concentration, green dots: NO_x concentration, blue dots: wet deposition NO_y, NH_x, red dots: dry deposition NH_3.

2.2 Inverse Modeling Method

Comparing the OPS modelling concentration and the observation data, the model can be optimized.

State

Now that we have the observation data y, the original emission estimate x_a and the forward model F (the model parameters were omitted for simple notation), we can improve the performance of the model by so-called inverse modeling analysis. According to Brasseur *et al.* (2017), inverse analysis helps us to find the optimal emission estimate $\hat{x}$, by reducing the errors in the forward simulation $y = F(x)$. The process in inverse analysis involves building the Jacobian matrix and minimizing the cost function of the forward model.

Error Reduction

Concerning the emission sources releasing NH_3 to the atmosphere, each of them has an emission rate x together with an emission error ε_x. Thus, the original estimate can be noted as $x_a + \varepsilon_{x,a}$. Similarly, there can also be a difference between the measured concentration y and the model simulation $F(x)$. We note it as the observational error ε_o. It can be further divided into three components: $\varepsilon_o = \varepsilon_I + \varepsilon_M + \varepsilon_R$. The instrument error ε_I is the error between the measured value and the real concentration during the measurement process. The model error ε_M is the error contributed by the model parameters such as winds and model physics. It occurs during the forward model simulating the concentration. The representation error ε_R describes the mismatch between the model resolution and the measurement location. It is caused by the numerical discretization of the model equations. In inverse modeling, ε_I and ε_M are in an inherent relationship. A very precise instrument is useless if the model is poor; on the contrary, a good performing model is useless if the instrument measures roughly. Instrument and model must match well if we want to obtain a better knowledge of x from y (Brasseur *et al.*, 2017).

In this research, both the emission estimate x and observations y are vectors. The dimensions correspond to the numbers of emission categories and receptors respectively. As a result, the errors are all vectors as well. To solve the inverse problem requires the construction of the prior emission error covariance matrix $S_x = [\varepsilon_x \varepsilon_x^T]$ and of the observational error covariance matrix $S_o = [\varepsilon_o \varepsilon_o^T]$ as input of the calculation. The errors are assumed uncorrelated so that S_o is the sum of the instrument error covariance matrix $S_I = [\varepsilon_I \varepsilon_I^T]$, the representation error covariance matrix $S_R = [\varepsilon_R \varepsilon_R^T]$, and the forward model error covariance matrix $S_M = [\varepsilon_M \varepsilon_M^T]$: $S_O = S_I + S_R + S_M$ (Brasseur *et al.*, 2017).

Bias of the error

The observational error could be biased if the instrument is inaccurate or if there are systematic errors in some aspect of the forward model. The bias will be propagated through the equations to cause a corresponding bias in the solution. In that case, the observation bias is rewritten as

$$y = F(x) + b_o + \varepsilon_o'.\ b_o = E[\varepsilon_o]$$

ε_o' is the residual random error such that $E[\varepsilon_o'] = 0$. The optimal estimate can be derived as above by replacing y with $y - b_o$ (Brasseur *et al.*, 2017).

Description and building Jacobian Matrix

The prior emission estimate used here is assumed to be a unit multiplier for each selected category. In other words, after the optimization, all sources within this category will be multiplied by the optimized multiplier. The prior multipliers for all categories make up an original estimate vector $x_a = [1, 1, \cdots 1]$. From previous section, we know the OPS model is linear. Therefore, we can assume the model expression as: $F(x) = Kx$. *K* is the so-called Jacobian Matrix describing how weights each emission element in the projection to *F(x)*. It can be constructed by changing the input of certain elements and observing the consequent results.

If we make a perturbation d_x to the original input x_a, the Jacobian matrix is calculated as: $K = (F(x_a + d_x) - F(x_a))/d_x$. With the fact that the model is linear, the process can be simplified by doing separate runs for the emission of one category only and setting the d_x as a unit prior value of the multiplier. Thus, the result of a separate run $C_{contr,i}$ equals to the corresponding column of the Jacobian Matrix, as: $K_i = C_{contr,i}$ (Figure 6).

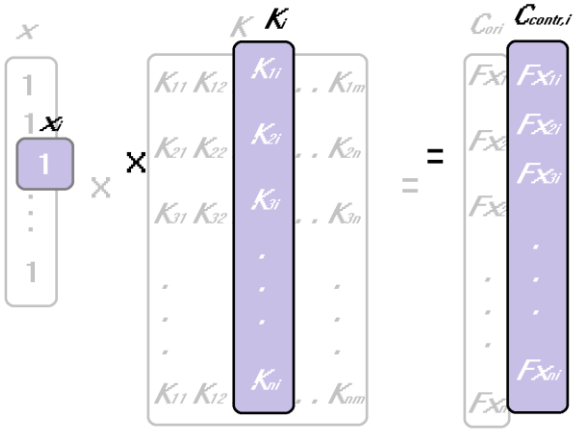


Figure 6 The building of Jacobian Matrix K. According to the linearity of the model, the column K_i equals to the corresponding contribution concentration $C_{contr,i}$, $K_i = C_{contr,i}$.

Calculation of Cost Function

Now that we have prepared the observation vector y, the prior information x_a, the forward model F, and the error covariance matrices S_x and S_O, the optimal estimate $\hat{x}$ can be calculated. According to Brasseur *et al.* (2017), $\hat{x}$ is obtained when the cost function $J(x)$ attains its minimum value. $J(x)$ reflects the observational and emission error constraints to the model, showing the maximum conditional probability density of x when y has a known value. The equation to calculate it is:

$$J(x) = (x - x_a)^T S_x^{-1}(x - x_a) + \big(y - F(x)\big)^T S_o^{-1}(y - F(x))$$

To find its minimum, the derivative of it should be 0, or $\nabla_x J(x) = 0$:

$$\nabla_x J(x) = 2S_x^{-1}(x - x_a) + 2K^T S_o^{-1}(F(x) - y) = 0$$

$K^T = \nabla_x F^T$is the transpose of the Jacobian matrix. Considering the OPS model is a linear model, the optimal estimate can be expressed as:

$\hat{x} = x_a + G(y - Kx_a)$,

with

$G = S_x K^T (KS_x K^T + S_o)^{-1}$ is the gain matrix, which shows the sensitivity of the optimal estimate to the observations, i.e., $G = \partial\hat{x}/\partial y$. In inverse modeling, it tells us which observations contribute most to constrain specific components of the optimal estimate.

The optimal error covariance matrix of $\hat{x}$ is calculated as:

$$\hat{S} = (K^T S_o^{-1} K + S_x^{-1})^{-1}$$

2.3 Experiment Design

According to the research questions, OPS model features and the method of inverse modelling, the experiment can be described in the following steps:

- Some pre-simulations are made to check the linear relationship between emission and concentration and to select the emission categories for analysis.
- Given the emission data and categories, we will simulate the ammonia concentration in the Netherlands for a one-year period. Then we compare the yearly average result with the observed concentration in order to check OPS's performance.
- Changes are then made for a certain emission source category, while the others are fixed. We analyze how the change in each emission category affects the concentration (to construct the Jacobian matrix).
- Finally, we will try to optimize emissions in the different categories, to find a best match between model and observations (inverse modelling); To avoid unrealistic solutions, realistic lower and upper boundaries for each emission category must be provided to the system, in the form of matrices S.
- We will test the sensitivity of the result to different assumptions of the assumed model error, and will also investigate the effect of possible model biases.

Linearity of the model

The linearity of the model is checked in this research by a simulation with 2 receptors and different emission inputs. In addition, to test if there are bias in the model or original NH_3 preset in the air, a run without emissions was also made. Since the model cannot run with all zero input values, one of the 1.08×10^6 emission sources are set to be $1 \times 10^{-10} g/s$. The average simulated concentration was almost zero ($0.593 \times 10^{-15} \mu g/m^3$). Therefore, we can confirm $c = 0$ in the linear equation $F(x) = kx + c$.

Emission input

For this research, the emission input consists of files with 832475 emission sources in the Netherlands and 251815 sources in the surrounding countries and the sea (available on www.emissieregistratie.nl). The emitting time is a one-year period in 2018. For some sources of the outside, due to the lack of recent census, data of 2017 is used instead. The emission sources can be generally divided into 8 categories, namely Industry, Energy, Vehicles, Agriculture, Waste Processing, Commerce, Construction and Consumers. Each of them can be further divided into detailed categories and the codes are in the appendix A. Among the categories, the agriculture is expected to be the major emission source. A test run was operated to verify the contribution of each category. After that the agriculture emission was further divided into stable animals (including some major livestock kinds and others), storage of livestock, manure application of different animals on the fields, fertilizers use (including compost and inorganic *N* fertilizers), emission from standing crops, crops residues and fires. Traffic and consumers emission are also two important emission sources, so they were kept separate categories. The other categories were combined as one due to the low emission amount. Emissions from surrounding countries, Belgium and Germany, together with the sea were set as independent categories, while the *NH₃* transported from all further countries was in one category.

Error of the experiment

The emission error ε_x in the Netherlands is related to each emission category (Table 1), which can be found in Lagerwerf *et al.*, 2019. One standard deviation is used for this study. For those categories that are not in the list or for emissions from other countries, a default value of 15% is assumed, while emissions in Belgium and Germany are assumed with 30% uncertainty due to close distances and interactions. The measuring instrument error ε_I is made up of an absolute value and a relative part depending on measured concentration by each receptor, as $[0.1^2 + 0.096^2 \times conc^2]^{0.5}\ \mu g/m^3$ for annual standard uncertainty (Lolkema *et al.*, 2015). There is no reference available for the model error ε_m. Based on the results of modeling, we tried 0.35, 1 and 4 $\mu g/m^3$ respectively for the model error. Since the OPS model computes

concentrations directly at the location of the measuring stations, the representative error is omitted in this research and assumed to be included in ε_m.

Table 1 Relative emission error of each category (Lagerwerf *et al.*, 2019). One standard deviation is used for this study.

Emission Category	Relative Emission Error (%)
Stables: dairy cattle	20.5
Stables: Other cattle	16
Stables: Breeding pigs	18.5
Stables: Fattening pigs	21
Stables: Poultry laying hens	21
Stables: Other poultry	24.5
Stables: Other livestock	25
Livestock storage	23.5
Grazing: dairy cattle	55
Grazing: other livestock	45
Manure use: grazing animals	34.5
Manure use: stable animals	40
Manure processing	11.5
Fertilizer application	30
Crops and fires	30
Traffic	15
Consumers	15
Other categories	15
From Belgium	30
From Germany	30
From other countries	15
From the sea	15

3. RESULT

3.1 Emission Analysis

3.1.1 Emission Distribution

Figure 7 shows the NH_3 emission over the Netherlands and the nearby countries. Emission data has a higher resolution within the Netherlands. There are obviously more hotspots in the east part of the Netherlands than in the west, especially the grassland areas in Friesland, east Gelderland and between North-Brabant and Limburg. It can be noticed that there is less emission from the coastal city areas and low value from the forests in the central Gelderland and the east part of Utrecht. However, there was a hotspot with very high emission between those forest areas (Gelderse Vallei). Concerning the surrounding regions, it also can be found that the emission in cities has lower emission, like Brussel in Belgium and Rhine-Ruhr metropolitan region in Germany. On the contrary, more hotspots occurred in rural areas, like northwest Germany and the coastal region in Belgium. Different from that in the continent, the emission from the sea was low and evenly distributed. Given the large area, the total amount is still non-negligible (~1050 g/s in the sea nearby).

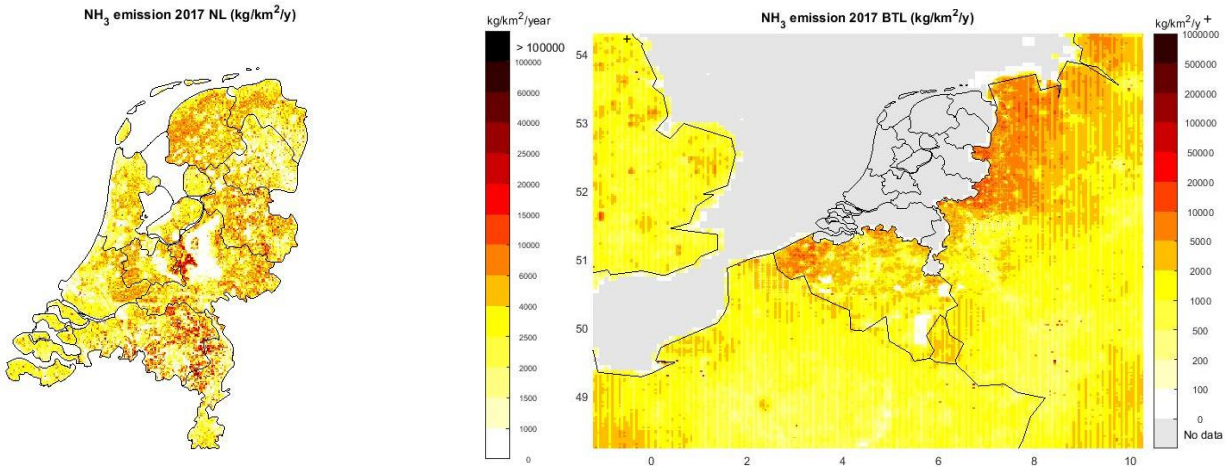


Figure 7. Emission of NH_3 in the Netherlands (right) and the sea and the surrounding countries (left), in 2017.

With the knowledge of the emission sources special distribution, we can look further into different emission categories. The histogram below presents the NH_3 emitted from each category within the Netherlands (Figure 8). We find that grazing animals' manure use has the largest amount of emission (1030g/s) in the Netherlands as a total. This category is also assigned the largest error (350g/s). The following most influential emission in agriculture is from dairy cattle with around 880g/s and 150g/s uncertainty. The other agricultural emissions are much smaller. Other obvious stable categories

are fattening pigs (~300g/s) and laying hens (~190g/s). However stable animals manure use on cropland has only 205g/s emission. More NH_3 was emitted from fertilizers (~320 g/s). Besides emissions from agriculture, NH_3 emission from traffic (~170g/s) and consumers (~380g/s) is important.

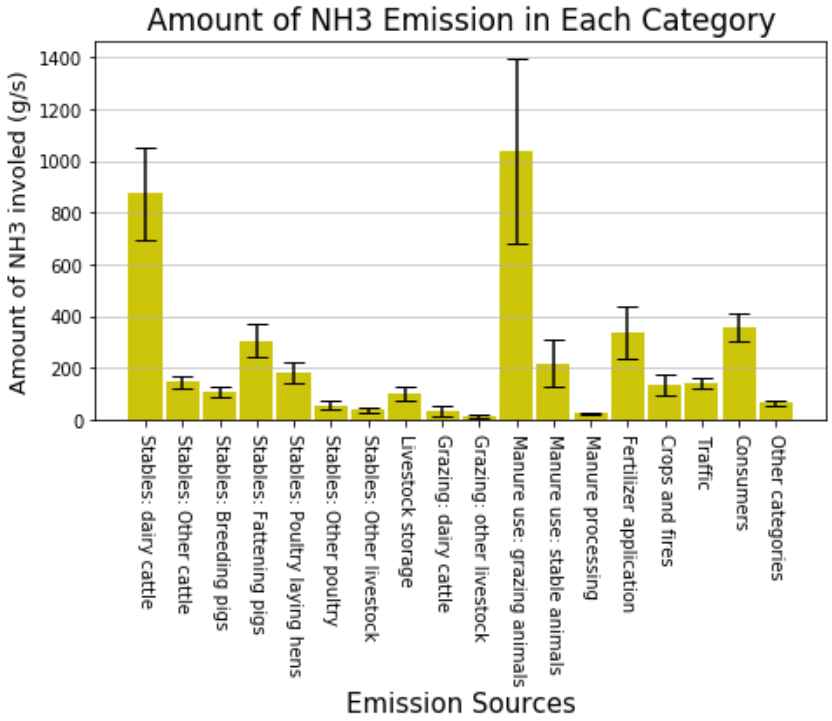


Figure 8 Each category's ammonia emission rate within the Netherlands.

Compared with the domestic emission sources, NH_3 that is emitted outside the Netherlands needs to travel a long distance to enter the Netherlands. However, with a huge total amount from the countries nearby, the effect could be important as well, especially for regions close to the border. For this reason, the domestic emission, foreign transport, and emissions from the sea are all taken into account when simulating NH_3 concentration.

3.2 OPS Simulation

3.2.1 Comparison with the Observation

With the emission data as the input, OPS modelling results are available for analysis. Figure 9 shows a comparison between the modelling result and the observation data. The OPS model has an acceptable performance on simulating the NH_3 concentration in 2018. The points of a scatter plot are located close to the 1:1 line. The Correlation Coefficient (R) equals to 0.84 and Cost-function was 450.08. It can be noticed that the low-value observations (~0-5 $\mu g/m^3$) are generally underestimated by the OPS model.

More points are located above the 1:1 line when the concentration is higher (~10-15 $\mu g/m^3$), showing the overestimation of the model in this concentration range. Concerning the uncertainty, we can see the points have larger error bars as the concentration are higher. This was reasonable because there were relative components in the calculation of observational error (from the equation). Another finding is that the simulation of NH_3 concentration on the LML receptor points (orange) is more scattered than for the MAN receptor points (blue).

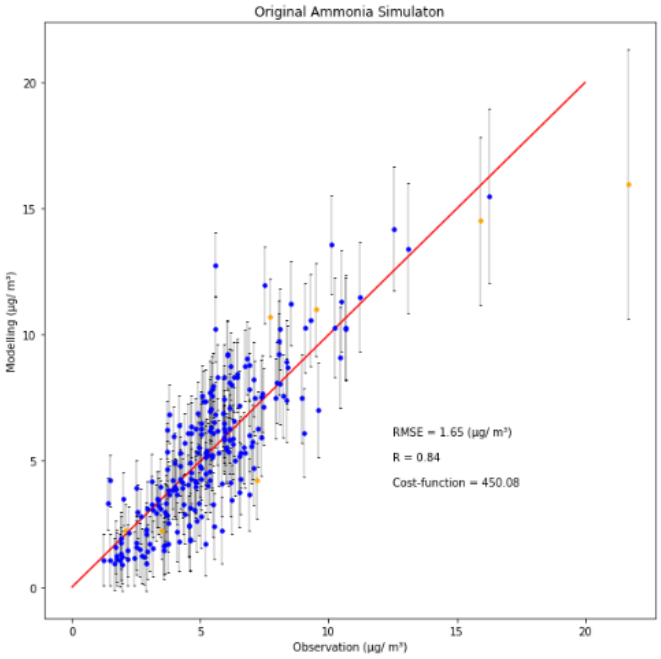


Figure 9 Scatter plots between the simulation and the observation of MAN measurement system (blue points) and LML measurement system (orange points) in 2018. The red line is the 1:1 reference line.

3.2.2 Atmospheric concentration of NH_3 *in NL*

The OPS model simulates the NH_3 concentration around the measurement stations. Figure 10 gives information about the spatial variation of NH_3 concentration over the Netherlands. It is obvious that the eastern part of the Netherlands has much higher concentrations than the west. Especially in the eastern part of the province North-Brabant and southern Overijssel, many stations show high concentrations of NH_3 in the air. Another hotspot is the area with a concentration of poultry farms, east of Utrecht city. Consistent with the emission distribution, the concentrations in South-Holland and the central forests are relatively low. This pattern is caused by the main circulation, with predominant winds from the south-west.

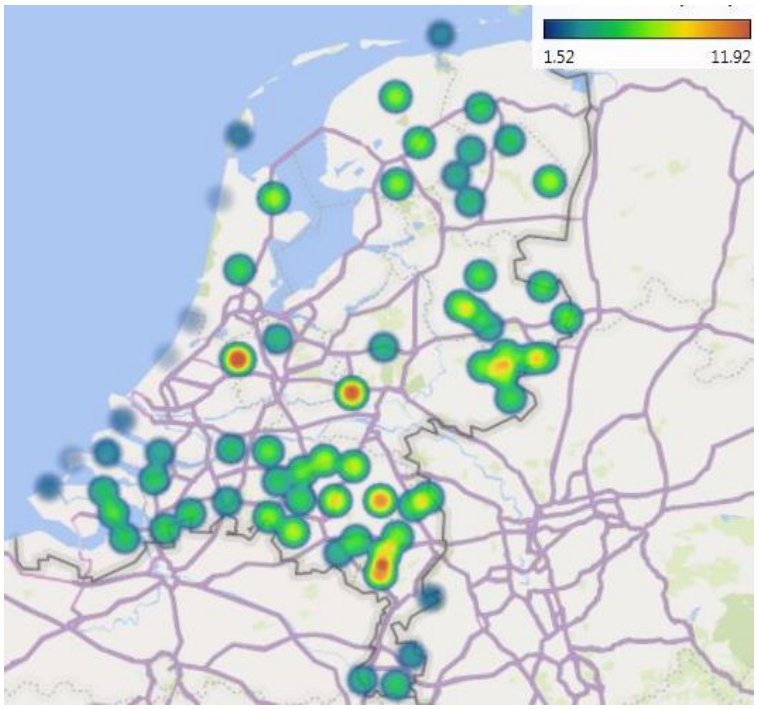


Figure 10 Modelled *NH_3* concentration at measurement stations in the Netherlands in 2018 (in $\mu g/m^3$). The points are located where the stations are.

3.2.3 Contribution of each category in NH_3 *concentration*

A fraction of emitted *NH_3* will deposit back to the ground, react into secondary products, or transport outside and the other part remains in the air. To study the contribution of different emission sources, the percentage from each category in the average *NH_3* concentration is calculated. Note that this is the average over all measuring stations and not the average over the Netherlands as a whole. As shown in Table 2, dairy cattle are the most important source (23.3%). Other cattle (4.9%) and fattening pigs (9.4%) also have relatively high contributions, which is in line with their emission strength (Figure 11). However, despite the high emissions of grazing animals' manure use (~24.8% of domestic emission), only 9.3% of *NH_3* in the air is from this category. A similar low contribution is observed in other manure-related categories. Fertilizer use, crop emission and fires on cropland also had low contribution rate compared with their emission amount. In contrast, 10.7% of the *NH_3* is originating from consumers, which was very high compared with its emission amount (8.6%). In addition, *NH_3* that is transported from outside of the Netherlands also contributes a lot. Germany (10.4%), Belgium (4.2%) and the sea (4.4%) were critical sources, while countries further away only contributed around 0.6% together.

Table 2 Emission percentage of each category, and after deposition, chemical reaction and in- and out-fluxes, the concentration percentage originated from each category. The NH_3 concentration from outside is the result of transportation.

Emission Category	Emission (%)	Concentration (%)
Stables: dairy cattle	20.9	23.3
Stables: Other cattle	3.5	4.9
Stables: Breeding pigs	2.5	3.2
Stables: Fattening pigs	7.3	9.4
Stables: Poultry laying hens	4.3	4.8
Stables: Other poultry	1.4	1.6
Stables: Other livestock	0.9	0.9
Livestock storage	2.4	2.6
Grazing: dairy cattle	0.8	0.4
Grazing: other livestock	0.3	0.1
Manure use: grazing animals	24.8	9.3
Manure use: stable animals	5.2	2.2
Manure processing	0.6	0.8
Fertilizer application	8.1	2.9
Crops and fires	3.3	1.0
Traffic	3.4	1.6
Consumers	8.6	10.7
Other categories	1.6	0.5
From Belgium		4.2
From Germany		10.4
From other countries		0.6
From the sea		4.4

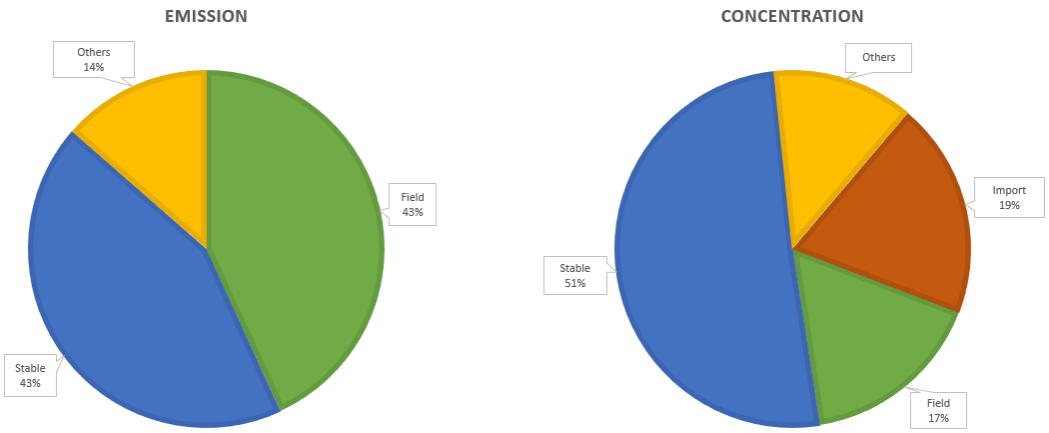


Figure 11 Emission percentage and after deposition, chemical reaction and in- and out-fluxes, the concentration percentage originated from different categories. The NH_3 concentration from outside is the result of transportation. Pie charts for each category are in Appendix II

3.3 Model Optimization

The OPS simulation result gives us information about different NH_3 emission categories and regions and how they influence the atmospheric concentration in the Netherlands. By reducing the errors with the inverse modelling method, the model is optimized, and a new emission estimate is obtained, with reduced uncertainty. No bounds are imposed on the new emission estimate.

3.3.1 Performance Improvement

A comparison between the performance of the original and the optimized simulation is shown in Figure 12. After the optimization, it is found that the points further approach the 1:1 reference line, which means the OPS modelled concentrations are closer to the observation values. The Correlation Coefficient (R) increased from 0.84 to 0.88. As a result of error reduction, the Cost-function $J(x)$ decreases from 450.08 to 285.90. Note that this value is by definition the minimum cost function that can be obtained given the current settings.

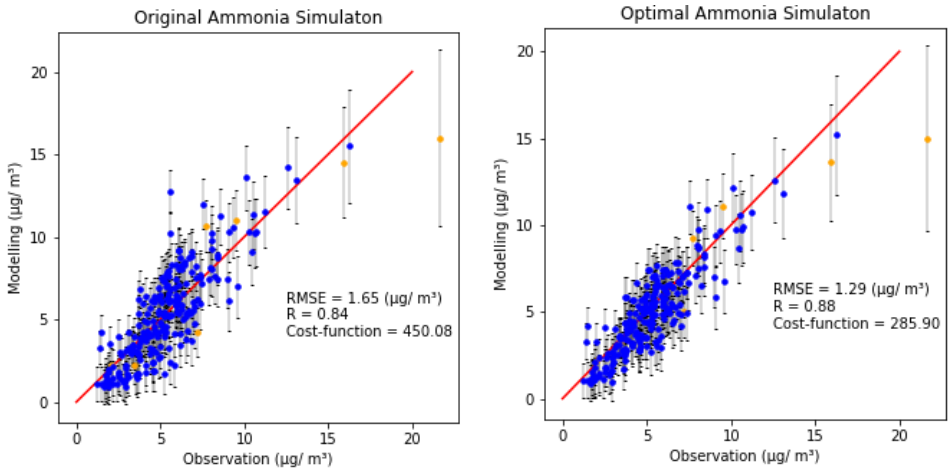


Figure 12 Original (left) and optimized (right) scatter plots between the simulation and the observation of MAN measurement system (blue points) and LML measurement system (orange points). The red line is the 1:1 reference line.

3.3.2 Optimized Emission Estimate

Figure 13 and Table 3 show the optimized emissions of the different categories, scaled to the original value ($x_a = 1$). The histogram height presents the relative change in emissions. An overestimation (~5-25%) is prevalent for stable animals, while the estimates mostly remained the same for grazing animals. The manure use of both stable and grazing livestock is underestimated according to the calculation. Especially for stable animals' manure, the optimized emission is more than 1.8 times larger than the original value. Underestimation is also observed for fertilizer application (25%) and crops and fires (40%). Traffic emission becomes ~2% higher and that of consumers becomes ~10% lower. In terms of foreign emissions, a significant underestimation of 50% and overestimation of 50% is calculated for Belgium and Germany, respectively.

The black error bars denote the reduced emission uncertainty and the red bars behind them were the original emission errors. As shown in Figure 13, significant error reduction occurs in the category of dairy cattle, manure use: both stable and grazing animals, and consumers. Stable animals' manure use was the emission category with the largest change, and the other three are the major NH_3 sources in the Netherlands. Other categories with obvious lower emission errors are fattening pigs, NH_3 transported from Belgium, Germany and the sea. For certain important categories, like grazing animals and crops and fires, the error was almost not reduced.

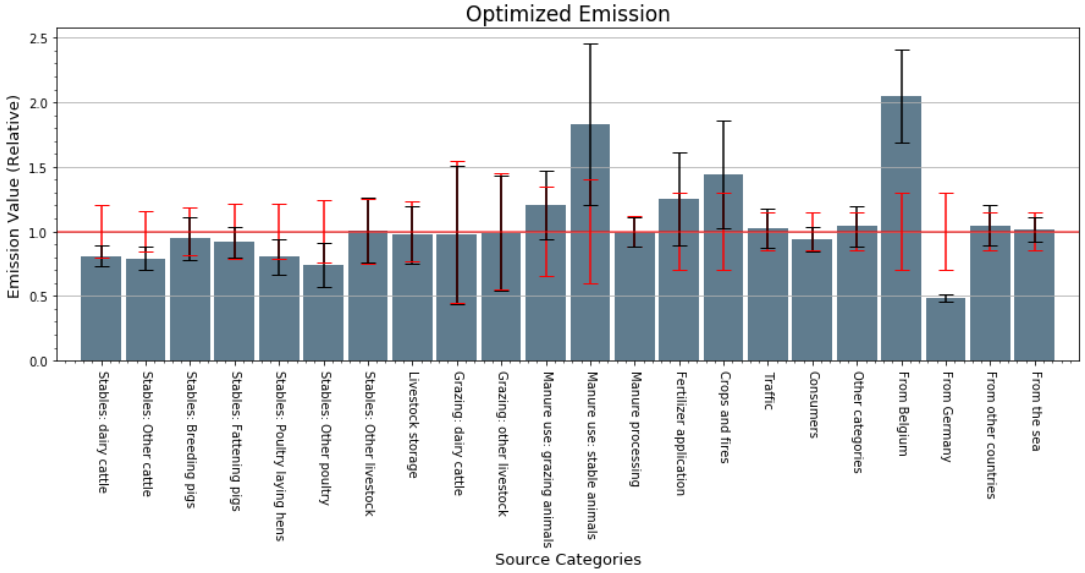


Figure 13 The relative changes in the emission estimate and error. The original value of all categories was 1 (the red line) and the optimal estimate values were the heights of the columns. The red error bars were the corresponding original emission errors and the black error bars were the error after reduction.

Table 3 Emission amount of each category and its uncertainty before and after the optimization

Emission Category	Original Emission (g/s)	Optimized Emission (g/s)	Original Emission Error (%)	Optimized Emission Error (%)
Stables: dairy cattle	873.5	706.6	20.5	10.1
Stables: Other cattle	146.5	115.8	16	11.5
Stables: Breeding pigs	105.6	100.0	18.5	17.7
Stables: Fattening pigs	304.0	279.1	21	12.8
Stables: Poultry laying hens	181.8	145.8	21	17.7
Stables: Other poultry	57.1	42.3	24.5	22.6
Stables: Other livestock	39.0	39.3	25	24.8
Livestock storage	101.3	98.7	23.5	22.7
Grazing: dairy cattle	34.7	33.9	55	54.8
Grazing: other livestock	11.9	11.7	45	45.0

Manure use: grazing animals	1037.3	1249.2	34.5	21.8
Manure use: stable animals	219.2	401.2	40	34.1
Manure processing	26.8	26.7	11.5	11.5
Fertilizer application	338.0	422.9	30	28.7
Crops and fires	136.0	196.1	30	29.1
Traffic	141.3	144.9	15	14.8
Consumers	358.7	337.2	15	10.0
Other categories	67.7	70.3	15	15.0
From Belgium	2.2E+03	4.4E+03	30	17.5
From Germany	2.1E+04	1.0E+04	30	6.7
From other countries	1.6E+05	1.7E+05	15	15.0
From the sea	1.0E+03	1.1E+03	15	9.3

3.3.3 Bias Correction and Model Error

Bias correction

According to the bias correction method and the situation of this research, 3 types of bias correction cases were used for correction during the optimization.

1) $b_o = \bar{y} - \overline{F(x_a)}$, 2) $b_o = \sum \frac{y_i - F(x_a)_i}{S_{o,i}} / \sum S_{o,i}^{-1}$, 3) without bias.

For the first type, the average value of all receptors is used. In comparison, the second type calculates the bias of each receptor separately and includes the error for every element of the vector. After the bias correction, the original model performs better than before (Table 4). The improvement is less so that the optimized model performs slightly poorer, as the corrected result had higher cost function than that without bias correction. There was no obvious difference in the results between the 2 bias calculation methods.

Table 4 Optimizing results before and after bias correction

		Without Correction	With Bias Correction 1	With Bias Correction 2
Original	RMSE	1.74	1.65	1.65

	R	0.84	0.84	0.84
	Cost Function	502.94	450.08	450.08
Optimal	RMSE	1.22	1.28	1.28
	R	0.89	0.89	0.89
	Cost Function	244.67	280.79	280.74

Optimized estimate with different model errors

When the model error is changed to a different value, corresponding change is on the optimized emission estimate. As shown in Table 5, some categories are not sensitive to the uncertainty changes, like cattle and pigs, livestock storage and traffic. On the contrary, for other categories like other poultry, manure use, crop and fires, the changes are larger. This shows the simulation of NH_3 from these categories may be more complicated. We can also find for categories that change a lot after the optimization, such change will be enlarged significantly by the small model error. Example is like transportation from Belgium and Germany, or manure use of stable animals.

Table 5 Optimized estimate (emission multipliers) with the model error of 1, 2 and 0.6 $\mu g/m^3$.

Emission Category	**1 $\mu g/m^3$**	**2 $\mu g/m^3$**	**0.6 $\mu g/m^3$**
Stables: dairy cattle	0.81	0.87	0.80
Stables: Other cattle	0.79	0.88	0.74
Stables: Breeding pigs	0.95	0.98	0.91
Stables: Fattening pigs	0.92	0.99	0.85
Stables: Poultry laying hens	0.80	0.90	0.75
Stables: Other poultry	0.74	0.90	0.59
Stables: Other livestock	1.01	1.00	1.01
Livestock storage	0.97	0.99	0.99
Grazing: dairy cattle	0.98	0.99	0.95
Grazing: other livestock	0.99	1.00	0.96

Manure use: grazing animals	1.20	1.10	1.22
Manure use: stable animals	1.83	1.40	2.13
Manure processing	1.00	1.00	0.99
Fertilizer application	1.25	1.11	1.37
Crops and fires	1.44	1.18	1.71
Traffic	1.03	1.01	1.05
Consumers	0.94	1.01	0.85
Other categories	1.04	1.01	1.08
From Belgium	2.05	1.58	2.29
From Germany	0.48	0.52	0.48
From other countries	1.05	1.02	1.08
From the sea	1.02	1.04	0.96

4 DISCUSSION

4.1 Result Analysis

Stable and storage

Emission from livestock stable and the storage inside and outside the stable are one of the dominant NH_3 sources. NH_3 is mainly released from the urine excreted by animals in the stables and the mineralized organically bound N in mammals feces also contribute a small amount (Lagerwerf *et al.*, 2019). Although the latest calculation method using total ammoniacal N (TAN) instead of total N excretion (Oenema et al., 2000; Van der Hoek, 2002) avoids much overestimation, some emission loss can still exist, like the TAN loss as gaseous N compounds (Vonk *et al.*, 2019). This might partially have led to the overestimation shown by the OPS model result. Other possible emission factors causing the overestimation and uncertainty include the number of animals per category, the proportion of organic *N* mineralization, different manure management systems and lack of occupancy, etc. (Vonk *et al.*, 2019).

According to Asman *et al.* (1998), NH_3 concentration drops rapidly within the first 1–2 km from the sources, as a result of dry deposition. This also causes high spatial

variation in rural areas. The stables are widely located in the large areas of grassland in the central Netherlands (Figure 14). Therefore, the emission from stable animals contributed the most to a high average concentration of the whole country. This explains the result of emission amount (**Fout! Verwijzingsbron niet gevonden.**).

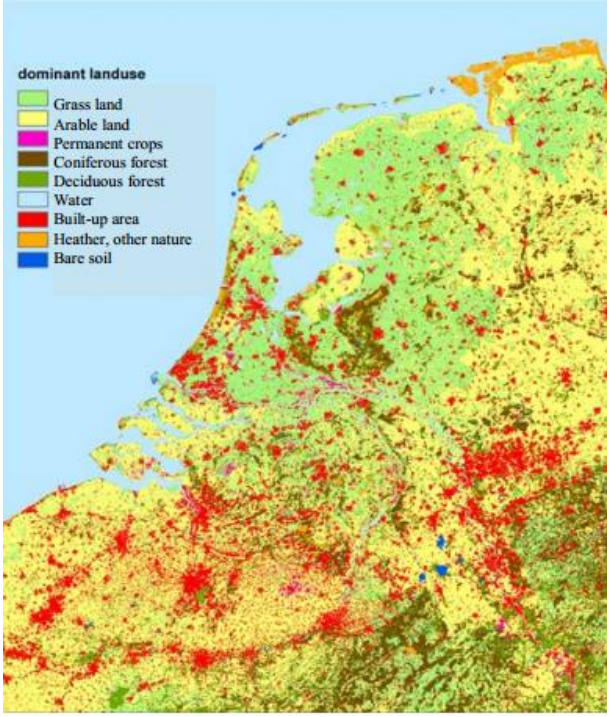


Figure 14 Dominant land use for the Netherlands and for Belgium and Germany (Sauter *et al.*, 2018).

Manure use and cropland

Another essential emission source is from the agricultural soil, including the manure application, crops emission and the excrement deposited by grazing animals. From the results, we found that the NH_3 emission from manure use is underestimated and the original errors are very high. Many emission factors might cause such a result, for example, the application techniques, the configuration of grassland, uncropped land, and cropland, or soil types (Vonk *et al.*, 2019). For the crops, the residue has relatively low emission uncertainty (20%), but the standing crop (150%) is hard to predict. Such uncertainties are hardly reduced by inverse modeling. The same problem happens for the category grazing animals as well.

Although the livestock manure is also applied in the grassland or other non-agricultural usage, the majority is used in the arable lands. From the previous chapter, we know that manure use emits a significant amount of NH_3. However, the croplands are

concentrated in the coastal region of Zeeland and the border areas of Groningen and Limburg (Figure 14). As shown in Figure 15, in the perspective of the one year, the wind is mainly from the south and west for most of the time. A large amount of NH_3 could have been transported out of the Netherlands. Together with dry deposition in the local area, it explains the relatively low proportion of NH_3 concentration originated to manure use (Table 2).

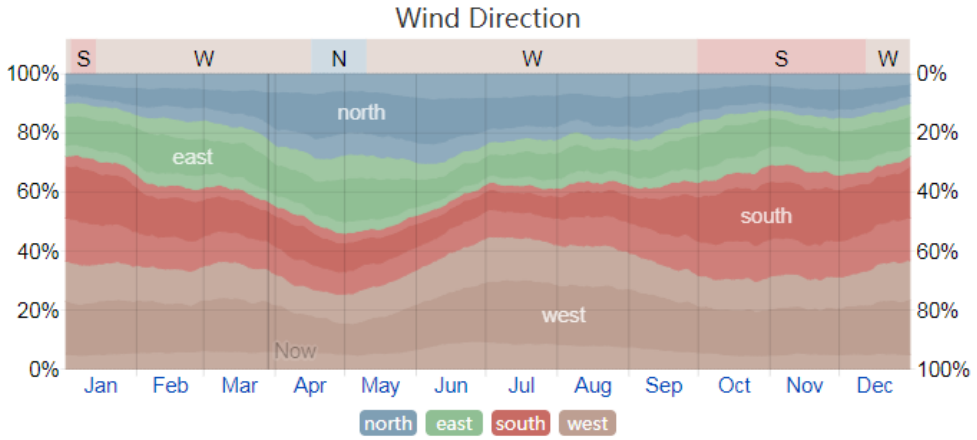


Figure 15 The annual percentage of hours in which the mean wind direction is from each of the four cardinal wind directions (based on a statistical analysis of historical hourly weather reports and model reconstructions from January 1, 1980 to December 31, 2016 observed in Amsterdam)(*Weather Spark*).

Traffic, consumers and other categories

The emission sources of these categories are generally located close to urban areas. The wind from the sea can transport the NH_3 emitted from the coastal cities eastward. Besides, the high mobility of traffic and consumers sources is likely to help the spreading. For some sources like industry, the relatively high emission height might have decreased dry deposition efficiency. Many of these NH_3 sources are also the sources of other pollutants or close to them (traffic, industry etc.). As a result, the NH_3 concentration is more sensitive to the change of acid gas (H_2SO_4, HNO_3, *etc.*) emission, which is more likely to cause under- or overestimation in the air. Especially more vehicles have the selective catalytic reduction systems in order to decrease NO_x emission, which can lead to an increase of NH_3 release (Sun *et al.*, 2017). According to Suarez-Bertoa *et al.* (2016), no regulation has been made so far, except for Euro VI standards for heavy trucks. Similar phenomenon also happens for the catalytic reduction equipment in power plants (Shah *et al.*, 2015).

Surrounding areas

Based on Asman *et al.* (1998), wet deposition caused by scavenging of particulate dominates inputs at remote locations far from sources. Water vapor aggregates around the aerosol (including NH_4^+) to form droplets. Gaseous NH_3 may then be easily absorbed on the surface and is then removed with the precipitation. Wind direction also plays a critical role in the NH_3 transportation from outside. The wind is prevalent from the south and west for the most time of the year, which means NH_3 is easier to be transported from Belgium than Germany. On the other hand, the high total amount of emission in Germany can still influence NH_3 in the Netherlands when the wind is from the east. The interaction between foreign countries and the boundary areas is also important. From the sections above we know there are underestimations on cropland emission that has large areas located in north-east close to the main emission region of Germany. The lower NH_3 export might lead to a corresponding higher import (Figure 13). Similarly, the overestimation of stable animal emission was likely to explain the change of emission from Belgium. Many stables are close to the southern border though there are also croplands in Limburg. The large difference after the optimization was also because of the high uncertainty. This is tested by setting the emission error to 15%, which reduces the optimized estimate of Belgium from 205% to 152% and from Germany from 48% to 54%.

4.2 Future Study

Bias Correction

For this study, we assume the emission and its error unbiased. But in reality, if ammonia emissions are under- or overestimated, the model may be systematically too low or too high, respectively. In this case, a bias correction would be undesirable. A bias-correction scheme is useful when biases are caused by factors outside the state, for instance, wind fields, atmospheric stability, etc. To further correct the bias in emission, emission data and analysis results from the other years are needed.

Model errors

To check the assumption of model error, simulations with assumed model errors are carried out. We find that with the higher model error, the optimized emission values stay closer to the original ones. In this case, we give less trust to the model so the boundaries for the emission factor become narrower consequently. If a category stays the same, and the error is not reduced, the measurement network does not provide enough information to constrain that source category. On the other hand, if the model

error is too low, the optimized result will change a lot by the other errors reduction. The result will be out of the preset boundaries and unrealistic. That might be out of the experience expectation because we overestimate the model's capability.

In the future study, if more information about the model error selection is available, we can give more precise emission estimates. For example, a relative model error that varies with the size of emission file or the number receptors can be used together with the absolute uncertainty.

Time and area resolved simulation

From the previous discussion, we know that the atmospheric concentration of NH_3 from emission estimate can be affected by certain emission factors, transportation, and efficiency of deposition. To further investigate the sensitivity of these factors, more controlled modelling runs are recommended.

For example, annual average values are used in this study but seasonal emission patterns significant influence the concentrations as well. Livestock manure emits more in the summer and more NH_3 is likely emitted by consumers in wintertime. Similarly, the meteorology changes in the year need to be considered. Because the NH_3 concentration has large spatial variation as the result of dry deposition, the distribution of sources is essential for the emission study. The original location of NH_3 also determines where it will be transported to. In the future, we could divide the Netherlands into different regions and vary the emission in each region. Simulations with such an extended optimization state in the future can give us more sensitivity information to improve the OPS model.

In Belgium and Germany, the emission estimate and the error in the sources might be different from those in the Netherlands. To further test the data of each category can be useful and we can estimate the transportation more effectively. Possible means maybe collecting more documents about how the emission is valued and conducting similar modeling of different categories in these areas.

Linearity of the model

The linear model makes the simulation process more efficient and the building of the Jacobian matrix easier. As a result, it is more capable for analyzing the estimation of

NH_3 emission and effects on the concentration. As the same time, there may also be some problems caused by the linearity. For example, the speed of chemical reaction between NH_3 and acid can be influenced by the NH_3 concentration. Similar efficiency changes may also occur in the deposition and transportation. More variables that depend on the NH_3 concentration are likely to improve the performance of the model in the future.

5. CONCLUSION

After simulating the NH_3 concentration in 2018 for one-year length based on the emission data and comparing the modeling result with the observation, we found the OPS model has a quite acceptable performance: the Correlation Coefficient equals 0.84 and the Cost-function is 450.08. The emission was divided into different categories according to the expected contribution of various emission sources. Through the method of inverse modeling analysis, the emission matrix (Jacobian) was constructed, which presents how the change of each emission source category affects the concentration. Then we optimized the model by reducing the errors to obtain the minimum cost-function value (285.90).

From the result, we showed that agricultural sources dominate the contribution to NH_3 concentration Within that the emission amount from stable livestock (including cattle, pigs and poultry) was overestimated and the NH_3 emitted from these categories had higher contribution to the concentration in the air. On the contrary, other essential emission sources from the cropland (including manure application and crop emission and fires) were underestimated and the contribution was relatively lower. Factors like manure application methods or changing numbers of animals made the emission estimation uncertainty very high for those categories. Other than agriculture, emission from traffic and consumers also had an influential contribution. The decline of acid in the air could reduce the amount of NH_3 to react with. The NH_3 transported from Belgium and Germany contributed 19.7% to the total concentration in the Netherlands. Emission from Belgium was significantly underestimated while that from Germany was overestimated a lot. Misestimation in the border areas and the high uncertainty could be the possible reasons.

Although the model performed well in the simulation of 2018 atmospheric NH_3, certain improvements are still needed. The linearity was checked in this research. It makes the analysis easier, but some processes may change with the NH_3 concentration. Data from other years can be helpful to correct bias. The better model error shall be set in future studies to let the model make the largest uncertainty reduction and keep within the realistic boundaries at the same time. Simulations, where emissions can be

changed regionally in the Netherlands, are needed to investigate detailed contribution and sensitivity. Also, time-varied simulations rather than yearly average are required. More information about foreign emission will be useful for better analysis of outside transportation as well.

6. REFERENCE

Asman, W. A. H., Sutton, M. A. and Schjørring, J. K. (1998) 'Ammonia: Emission, atmospheric transport and deposition', *New Phytologist*. Cambridge University Press, 139(1), pp. 27–48. doi: 10.1046/j.1469-8137.1998.00180.x.

Average Weather in Amsterdam, Netherlands, Year Round - Weather Spark (no date). Available at: https://weatherspark.com/y/51381/Average-Weather-in-Amsterdam-Netherlands-Year-Round (Accessed: 29 March 2020).

Behera, S. N. *et al.* (2013) 'Ammonia in the atmosphere: A review on emission sources, atmospheric chemistry and deposition on terrestrial bodies', *Environmental Science and Pollution Research*. Springer, pp. 8092–8131. doi: 10.1007/s11356-013-2051-9.

Bleeker, A. *et al.* (2009) 'Linking Ammonia Emission Trends to Measured Concentrations and Deposition of Reduced Nitrogen at Different Scales', in *Atmospheric Ammonia*. Dordrecht: Springer Netherlands, pp. 123–180. doi: 10.1007/978-1-4020-9121-6_11.

Bobbink, R., Hornung, M. and Roelofs, J. G. M. (1998) 'The effects of air-borne nitrogen pollutants on species diversity in natural and semi-natural European vegetation', *Journal of Ecology*. John Wiley & Sons, Ltd (10.1111), 86(5), pp. 717–738. doi: 10.1046/j.1365-2745.1998.8650717.x.

Brasseur, G. P. *et al.* (2017) *Inverse Modeling for Atmospheric Chemistry, Modeling of Atmospheric Chemistry*. doi: 10.1017/9781316544754.012.

Buijsman, E. *et al.* (1998) 'An automatic atmospheric ammonia network in the Netherlands set-up and results', *Atmospheric Environment*. Pergamon, 32(3), pp. 317–324. doi: 10.1016/S1352-2310(97)00233-1.

Fahey, K. M. *et al.* (2017) 'A framework for expanding aqueous chemistry in the Community Multiscale Air Quality (CMAQ) model version 5.1', *Geoscientific Model Development*. Copernicus GmbH, 10(4), pp. 1587–1605. doi: 10.5194/gmd-10-1587-2017.

Franchin, A. *et al.* (2018) 'Airborne and ground-based observations of ammonium-nitrate-dominated aerosols in a shallow boundary layer during intense winter pollution episodes in northern Utah', *Atmospheric Chemistry and Physics*. Copernicus GmbH, 18(23), pp. 17259–17276. doi: 10.5194/acp-18-17259-2018.

Horva Th, L. and Sutton, M. A. (1998) *LONG-TERM RECORD OF AMMONIA AND AMMONIUM CONCENTRATIONS AT K-PUSZTA, HUNGARY*, *Atmospheric Environment*.

Lagerwerf, L. A. *et al.* (2019) *Methodology for estimating emissions from agriculture in the Netherlands Calculations of CH 4 , NH 3 , N 2 O, NO x , NMVOC, PM 10 , PM 2.5 and CO 2 with the National Emission Model for Agriculture (NEMA); Update 2019*.

Lolkema, D. E. *et al.* (2015) 'The Measuring Ammonia in Nature (MAN) network in the Netherlands', *Biogeosciences*. Copernicus GmbH, 12(16), pp. 5133–5142. doi: 10.5194/bg-12-5133-2015.

Loubet, B. *et al.* (2009) 'Ammonia deposition near hot spots: Processes, models and monitoring methods', in *Atmospheric Ammonia: Detecting Emission Changes and*

Environmental Impacts. Springer Netherlands, pp. 205–267. doi: 10.1007/978-1-4020-9121-6_15.
Luesink, H. and Michels, R. (2018) 'Ammonia regulations near nature areas in Denmark and the Netherlands compared'. doi: 10.18174/445690.
Sauter, F. *et al.* (2018) *The OPS-model*. Available at: https://www.rivm.nl/media/ops/OPS-model.pdf (Accessed: 10 September 2019).
Schlesinger, R. B. and Cassee, F. (2003) 'Atmospheric Secondary Inorganic Particulate Matter: The Toxicological Perspective as a Basis for Health Effects Risk Assessment', *Inhalation Toxicology*. Taylor & Francis, 15(3), pp. 197–235. doi: 10.1080/08958370304503.
Shah, S. *et al.* (2015) 'Optimal Ammonia Injection for Emissions Control in Power Plants', *IFAC-PapersOnLine*. Elsevier B.V., 48(30), pp. 379–384. doi: 10.1016/j.ifacol.2015.12.408.
Suarez-Bertoa, R. *et al.* (2016) 'On-road measurement of NH3 and N2O emissions from a Euro V heavy-duty vehicle', *Atmospheric Environment*. Elsevier Ltd, 139, pp. 167–175. doi: 10.1016/j.atmosenv.2016.04.035.
Sun, K. *et al.* (2017) 'Vehicle Emissions as an Important Urban Ammonia Source in the United States and China', *Environmental Science and Technology*. American Chemical Society, 51(4), pp. 2472–2481. doi: 10.1021/acs.est.6b02805.
Sutton, M. A. *et al.* (2003) 'Establishing the Link between Ammonia Emission Control and Measurements of Reduced Nitrogen Concentrations and Deposition', *Environmental Monitoring and Assessment*. Kluwer Academic Publishers, 82(2), pp. 149–185. doi: 10.1023/A:1021834132138.
van der Swaluw, E. *et al.* (2011) 'Wet deposition of ammonium, nitrate and sulfate in the Netherlands over the period 1992–2008', *Atmospheric Environment*. Pergamon, 45(23), pp. 3819–3826. doi: 10.1016/J.ATMOSENV.2011.04.017.
Vonk, J. *et al.* (2019) *Methodology for estimating emissions from agriculture in the Netherlands-update 2018 Calculations of CH 4 , NH 3 , N 2 O, NO x , PM 10 , PM 2.5 and CO 2 with the National Emission Model for Agriculture (NEMA)*.
Wichink Kruit, R. J. *et al.* (2017) 'Modelling trends in ammonia in the Netherlands over the period 1990–2014', *Atmospheric Environment*. Pergamon, 154, pp. 20–30. doi: 10.1016/J.ATMOSENV.2017.01.031.
Womack, C. C. *et al.* (2019) 'An Odd Oxygen Framework for Wintertime Ammonium Nitrate Aerosol Pollution in Urban Areas: NOx and VOC Control as Mitigation Strategies', *Geophysical Research Letters*. Blackwell Publishing Ltd, 46(9), pp. 4971–4979. doi: 10.1029/2019GL082028.
van Zanten, M. C. *et al.* (2017) 'Trends in ammonia measurements in the Netherlands over the period 1993–2014', *Atmospheric Environment*. Pergamon, 148, pp. 352–360. doi: 10.1016/J.ATMOSENV.2016.11.007.

APPENDIX I. CODE OF EMISSION CATEGORIES

4200 Agriculture: fertilizer application: fertilizer application / plant protection products and harvests

4340 Agriculture: Emission from agricultural crops and fires

4511 Agriculture: livestock farming: Stables: Dairy cattle

4512 Agriculture: livestock farming: Stables: Other cattle

4513 Agriculture: livestock farming: Stables: Breeding pigs

4514 Agriculture: livestock farming: Stables: Fattening pigs

4515 Agriculture: livestock farming: Stables: Poultry laying hens

4516 Agriculture: livestock farming: Stables: Other poultry

4517 Agriculture: livestock farming: Stables: Other livestock

4520 Agriculture: livestock farming: Storage:

4531 Agriculture: livestock farming: Grazing: dairy cattle NH3

4532 Agriculture: livestock farming: Grazing: other livestock NH3

4541 Agriculture: livestock farming: Manure use: grazing animals

4542 Agriculture: livestock farming: Manure use: stable animals

4550 Agriculture: livestock farming: Manure processing

4340 Agriculture: Emission from agricultural crops and fires

4200 Agriculture: fertilizer application: fertilizer application / plant protection products and harvests

4340 Agriculture: Emission from agricultural crops and fires

3000 Traffic

8000 Consumers

12567 Other categories

56 From Belgium

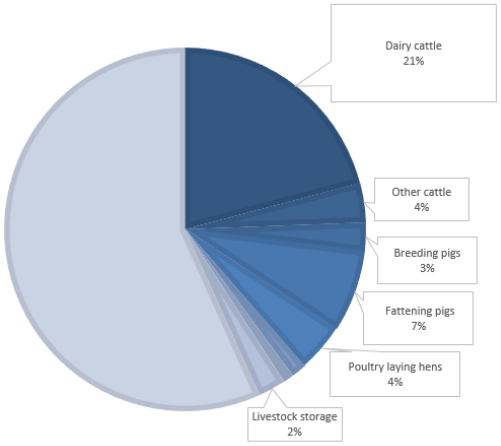
276 From Germany

998 From other countries

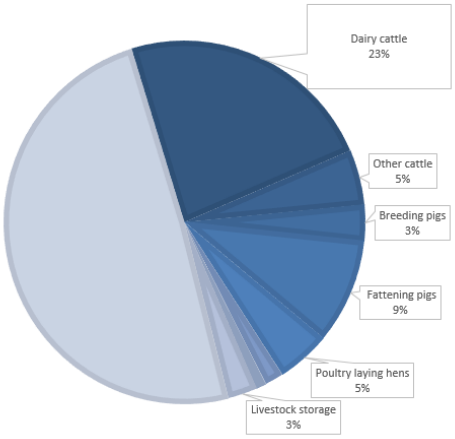
999 From the sea

APPENDIX II. EMISSION AND CONCENTRATION FOR EACH CATEGORY

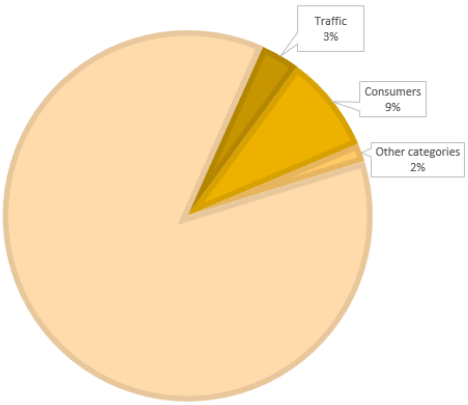
EMISSION



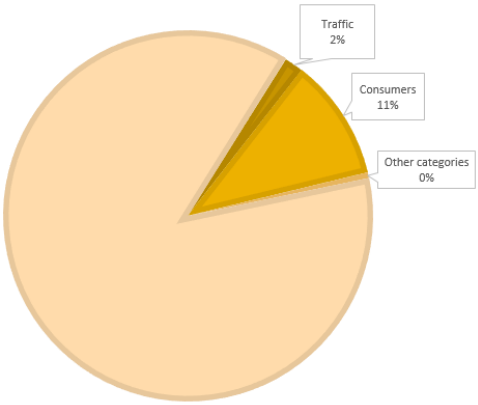
CONCENTRATION



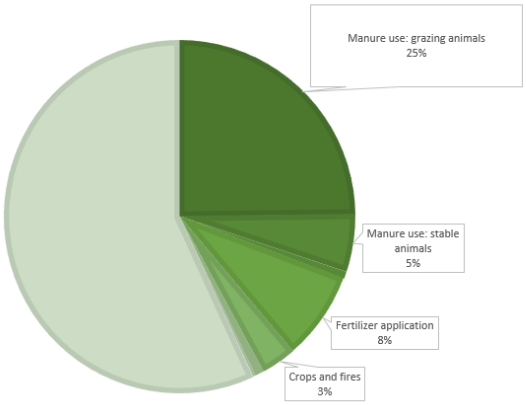
EMISSION



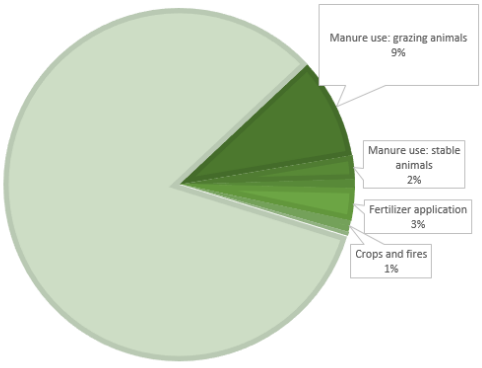
CONCENTRATION



EMISSION



CONCENTRATION



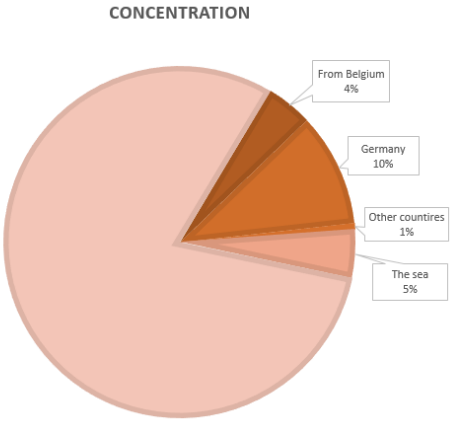


Figure 16 Emission percentage of each category, and after deposition, chemical reaction and in- and out-fluxes, the concentration percentage originated from each category. The NH_3 concentration from outside is the result of transportation.

APPENDIX III. PYTHON SCRIPT FOR EMISSION ESTIMATE OPTIMIZATION

```
import matplotlib.pyplot as plt
import numpy as np
import pandas as pd

# Based on Brasseur, Jacob    https://doi.org/10.1017/9781316544754.012
#>>>>>>>>>>>>>>>>>>>>>>>>>>>>>>>>>>>>>>>>CHOOSE                                    RECEPTOR
TYPE >>>>>>>>>>>>>>>>>>>>
```

```
def read_conc(filename, obs):

#Read OPS concentrations at LML or MAN locations

df = pd.read_csv(filename, skiprows=range(0, 3), header = None,
names = ['name', 'x', 'y', 'ammonia', 'dry', 'wet', 'tot', 'ammonium'],
delim_whitespace=True)

df = df.drop(['x', 'y', 'dry', 'wet', 'tot', 'ammonium'], axis=1)
df = df.sort_values('name')
df = df.reset_index()
df = pd.concat([df, obs], axis=1)
df = df.dropna()
output = df['ammonia']
#output = np.transpose(np.matrix(output))
return output

def compute_jacobian(rcp_type):

# Get observations:
obs = pd.read_excel('Observation.xlsx', sheet_name=rcp_type)

# Get reference concentration:
conc_ref = read_conc("Analysis/" + rcp_type + "/new_emission_result.tab",obs)

# n = number of receptors:
n = len(conc_ref)

# Create empty matrix
K = np.zeros(shape = (ncat, n))

# Loop over categories:
for icat in range(ncat):

# Read concentration for sensitivity run and compute Jacobian = dy/dx for this emission category
# dy/dx = (model(x=1) - model(x=0))/(1-0) = model(x=1), because model(x=0)= 0.
conc = read_conc("Analysis/" + rcp_type + "/" + rcp_type +"_" + str(categories[icat]) + ".tab",obs)
K[icat] = np.matrix(conc)
```

```
K = np.transpose(K)

# Skip missing values and get concentration values 'obs' and put observations into vector y:
obs = obs.dropna()
obs = obs['obs']
y = np.transpose(np.matrix(obs))



return K, y, conc_ref, n
#>>>
```

```
# model error covariance matrix:
S_m = np.diag(np.zeros(n) + err_model_abs**2)

# instrument error covariance matrix:
obs = np.squeeze(np.asarray(y))
delta_i_sqr_array = np.array(err_instr_abs +(err_instr_rel * obs)**2) # ug/m3
S_i = np.diag(delta_i_sqr_array)

# Observational error matrix; we assume that the representation error = 0,
# because OPS computes concentration directly at the location of the receptor:
S_o = S_m + S_i



#>>>>>>>>>>>>>>>>>>>>>>>>>>>>>>>>>>>>DEFINE THE LINEAR MODEL>>>>>>>>>>>>>>>>>>>>>
if iopt_bias == 0:
b_o = 0
elif iopt_bias == 1:
b_o = y.mean() - conc_ref.mean()
else:
b_o = sum((obs - conc_ref) / S_o.diagonal()) / sum(np.linalg.inv(S_o).diagonal())



def F(x):
# OPS-model (Taylor expansion around x_a):
F = K @ (x - x_a) + np.transpose(np.matrix(conc_ref)) + b_o
return F


#>>>>>>>>>>>OPTIMAL ESTIMATE (11.80 and 11.79 in Brasseur, Jacob)
#>>>>>>>>>>>>>>>>>>>>>>>>>>>>>
G = S_a @ np.transpose(K) @ np.linalg.inv((K @ S_a @ np.transpose(K)) + S_o)
x_optimal = x_a + G @ (y - F(x_a))
print ('The optimal x is:', x_optimal)


#>>>>>>>>>>>>>>>>>>>COST-FUNCTION (11.76, 11.77 in Brasseur, Jacob):
def cost(x):
```

```
J = np.transpose(x - x_a) @ np.linalg.inv(S_a) @ (x - x_a) + np.transpose(y - F(x)) @ np.linalg.inv(S_o)
@ (y - F(x))
return J


def cost_deri(x):
J_d = 2 * np.linalg.inv(S_a) @ (x - x_a) + 2 * np.transpose(K) @ np.linalg.inv(S_o) @ (F(x)    -y)
return J_d


#print('The original cost is:', cost(x_a))
#print('The optimal cost is :', cost(x_optimal))
#print('The optimal cost derivative is:', cost_deri(x_optimal))

# posterior error covariance matrix (11.81)
S_optimal = np.linalg.inv(np.transpose(K) @ np.linalg.inv(S_o) @ K + np.linalg.inv(S_a))
print('posterior error covariance matrix', np.sqrt(S_optimal.diagonal()))
```